Performance Analysis of Multi-Hop Hybrid FSO/mm Wave Communication System for Next-Generation Wireless Networks

Mogadala Vinod Kumar[1], Vinodh Kumar Minchula[2], M. Hemanth Kumar[3*], M Vamshi Krishna[4] and Sasibhushana Rao Gottapu[5]

[1]Department of Electronics and Communication Engineering, Dhanekula Institute of Engineering and Technology (A), Vijayawada,521139. India, mogadala.vinod@gmail.com
[2]Department of Electronics and Communication Engineering, Chaitanya Bharathi Institute of Technology(A), Telangana, India; vinodh.edu@gmail.com
[3]Department of Electronics Engineering, IIT (BHU) Varanasi 221005, Uttar Pradesh, India, mhemantkumar.rs.ece19@itbhu.ac.in
[4]Department of Electronics and Communication Engineering, Dhanekula Institute of Engineering and Technology, Vijayawada,521139, India, vamshi51@yahoo.co.in
[5]Department of Electronics and Communication Engineering, Andhra University College of Engineering, Visakhapatnam 530003, Andhra Pradesh, India, sasigps@gmail.com

*Correspondence: M. Hemanth Kumar; mhemantkumar.rs.ece19@itbhu.ac.in

ABSTRACT- Next-generation wireless networks are facing increasing demand for high data rates, low latency, and seamless connectivity. To address these challenges, a multi-hop hybrid communication system integrating Free Space Optics (FSO) and millimeter wave (mm Wave) technologies for backhaul communication is proposed. This system combines the advantages of FSO, such as high bandwidth and low latency, with the robustness and reliability of mm Wave technology. The multi-hop architecture enables the formation of a network of interconnected nodes, providing improved coverage and flexibility. Each node is equipped with FSO and mm Wave transceivers, allowing for seamless handovers and adaptive routing. For the proposed system, analytical formulas for outage probability (OP) and average bit error rate (ABER) are derived and validated using simulations. The Monte Carlo simulations provide evidence of enhanced performance in the proposed Multi-Hop Hybrid FSO/mm Wave (MHFM) system compared to the FSO system.

Keywords: Average BER, Free-Space Optics, Millimeter Wave, Multi-Hop, Hybrid FSO/mm Wave, Outage Probability.

1. INTRODUCTION

In the era of unprecedented connectivity demands and the emergence of data-intensive applications, next-generation wireless networks are required to deliver high-speed, low-latency, and reliable connectivity to the rapidly growing number of devices. The backhaul network, serving as the backbone of wireless communication systems, plays a pivotal role in meeting these requirements [1]. To address the ever-increasing demand for capacity and coverage, novel approaches must be explored to enhance the performance of backhaul links [2]. One of the key challenges in backhaul communication is the last-mile connectivity, which involves establishing reliable links between base stations and access points in a cost-effective manner. Traditional wired solutions such as fiber optic cables are often expensive and time-consuming to deploy, especially in rural and remote areas. Licensed microwave links, on the other hand, offer flexibility and scalability, making them an attractive alternative. However, these solutions face various shortcomings, including signal attenuation, interference, and capacity limitations.

Unlicensed millimeter wave (mm Wave) communications and free-space optics (FSO) are evolving as crucial technologies for enabling high data rates in future wireless networks. FSO operates in the optical spectrum, taking advantage of its inherent immunity to electromagnetic interference and abundant bandwidth availability [3]. By utilizing line-of-sight transmission, FSO offers a direct and secure connection with minimal latency [4]. On the other hand, mm Wave technology exploits the vast available spectrum in the millimeter-wave range to achieve multi-gigabit data rates, making it suitable for high-capacity backhaul links [5]. Multiple research papers [6, 7] have provided evidence that FSO transmission is significantly affected by fog but remains unaffected by rain. Conversely, mm Wave transmission is impervious to fog but susceptible to rain. The foundational basis for creating a hybrid FSO/RF system [8,9] arises from the divergent characteristics

of these technologies, enabling the exploitation of their respective strengths. However, it is widely recognized that FSO and mm Wave transmissions have limitations in terms of distance [10]. As the transmission distance surpasses 1km, the FSO communication system experiences a significant decline in performance attributed to environmental factors. Implementing a multi-hop transmission mode is seen to be an effective approach for achieving long-distance transmission and extensive coverage in FSO communication [11,12]. The multi-hop architecture is employed to extend the coverage range and improve link reliability [13,14]. In this approach, multiple FSO and mm Wave nodes are strategically deployed to create a relay network, allowing signals to traverse multiple hops before reaching the destination. Each node in the network acts as a relay, receiving the signal from the previous hop and forwarding it to the next, effectively extending the coverage area while mitigating the effects of atmospheric conditions and physical obstacles.

Therefore, inspired by the aforementioned information, here the MHFM system combining FSO, and mm Wave technologies is introduced. This study aims to evaluate the effectiveness of the proposed system through comprehensive simulations and analysis. We will assess key performance indicators, including outage probability (OP) and average bit error rate (ABER), under different channel conditions and environmental scenarios. The subsequent sections of this document are structured as follows. *Section 2* provides an overview of the system and channel model employed in the proposed scheme. Section 3 presents the derived statistical properties. *Section 4* discusses the performance analysis of the proposed system. *Section 5* presents the numerical results obtained from the simulations. *Section 6* summarizes the findings and outcomes of our study.

2. PROPOSED SYSTEM MODEL

The integration of FSO and mm Wave technologies, the use of relay nodes for multi-hop communication, and the overall system design is discussed in this section. Figure 1 illustrates the proposed system, which utilizes decode and forward (DF) relaying for multi-hop communication. The system comprises a source (S), a destination (D), and two relay nodes (R₁, R₂). The FSO connection stays active as long as its instant signal-to-noise ratio (SNR) surpasses a predetermined threshold. Meanwhile, the mm Wave link remains on standby. When the quality of the FSO link deteriorates and its instantaneous SNR drops below the specified threshold value, the receiver transmits a one-bit message to initiate the activation of the mm Wave link.

The same information signal is then transmitted across both FSO and mm Wave links with selection combining being used at the receiver after the data rate of the FSO link is decreased to the mm Wave link. In the suggested system, the initial relay node (R₁) is responsible for decoding the signal received from the source node (S) and subsequently relaying it to the relay node (R₂). After receiving the signal from node R₁, the node R₂ decodes it and subsequently transmits it to the destination node (D).
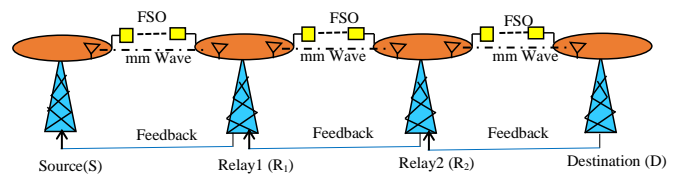

Figure 1: System model of hybrid FSO/mm Wave multi-hop

2.1 Mathematical Modelling of FSO Signals Received at Various Nodes

The signal received by node R_1 from node S in the case of an FSO link can be expressed as follows,

$$y_{SR_1}^{FSO} = c_{SR_1} I_{SR_1} g_{SR_1} x + n_{SR_1} \tag{1}$$

After decoding, the signal received by node R_1 is transmitted to node R_2. The signal received at node R_2 is given by,

$$y_{R_1R_2}^{FSO} = c_{R_1R_2} I_{R_1R_2} g_{R_1R_2} \tilde{x} + n_{R_1R_2} \tag{2}$$

The signal decoded by node R_2 is relayed to node D, and signal received at node D is given by,

$$y_{R_2D}^{FSO} = c_{R_2D} I_{R_2D} g_{R_2D} \hat{x} + n_{R_2D} \tag{3}$$

Where SR_1, R_1R_2, and R_2D are node S to node R_1, node R_1 to node R_2, and node R_2 to node D, respectively. c_j denotes the coefficient for converting optical signals to electrical signals at the receiver. I_j denotes the attenuation of the optical channel resulting from atmospheric turbulence in the jth connection. The node S transmits symbol x with an average energy E_s. Symbol $\tilde{x}$ denotes the estimate of x at node R_1, while symbol $\hat{x}$ represents the estimate of $\tilde{x}$ at node R_2. The average gain of the jth FSO link is represented by g_j. The noise (n_j) of the jth link is modeled as zero-mean circularly symmetric complex Gaussian. The noise n_j follows the property $E\{n_j n_j^*\} = \sigma_n^2$ and the value of $j \in \{SR_1, R_1R_2, R_2D\}$. The instantaneous electrical SNR at the FSO receiver's output is given by,

$$\gamma_j^{FSO} = \frac{c_j^2 g_j^2 E_s I_j^2}{\sigma_n^2} \tag{4}$$

The Log-Normal(L-N) distribution provides an effective characterization of the fading link in FSO communication, assuming ideal alignment between the transmitter and receiver, and the presence of weak atmospheric turbulence. The PDF of the fading channel coefficient (I_j) can be expressed as

$$f_{I_j}^{LN}(I_j) = \frac{1}{\sqrt{8\pi} I \sigma_x} e^{-\frac{[ln(I_j) - 2\mu_x]^2}{8\sigma_x^2}} \tag{5}$$

where, μ_x denotes the mean and σ_x indicates the variance of the L-N fading channel. In [15], it has been demonstrated that when E [I_j] = 1, it implies $\mu_x = -\sigma_x^2$. By combining *equations (4)* and *eq. (5)*, the equation for the PDF of the instantaneous signal-to-noise ratio of a Free-Space Optical link is given by,

$$f_{\gamma_j^{FSO}}^{LN}(\gamma) = \frac{1}{\sqrt{32\pi} \gamma \sigma_x} e^{-\frac{\left[ln\left(\frac{\gamma}{\gamma_j^{FSO}}\right) + 8\sigma_x^2\right]^2}{32\sigma_x^2}} \tag{6}$$

where, $\bar{\gamma}_j^{FSO}$ is the average SNR(ASNR) [15], and is given by,

$$\bar{\gamma}_j^{FSO} = \frac{c_j^2 g_j^2 E_s}{\sigma_n^2} e^{4\sigma_x^2} \qquad (7)$$

The cumulative distribution function (CDF) is obtained from the PDF of γ_j^{FSO} as

$$F_{\gamma_j^{FSO}}^{LN}(\gamma) = \int_0^{\gamma_j} f_{\gamma_j^{FSO}}^{LN}(\gamma)\, d\gamma \qquad (8)$$

The CDF of γ_j^{FSO} can be expressed using the complementary error function (erfc(x)) and error function (erf(x)) [19] as follows,

$$F_{\gamma_j^{FSO}}^{LN}(\gamma) = 1 - \frac{1}{2}\mathrm{erfc}\left(\frac{\ln\left(\frac{\gamma}{\bar{\gamma}^{FSO}}\right)+8\sigma_x^2}{\sqrt{32\sigma_x^2}}\right) \qquad (9)$$

2.2 Mathematical modelling of mm wave signals received at various nodes

The node R_1 receives the signal from the node S through the mm Wave link, and its expression is as follows,

$$y_{SR_1}^{mmW} = h_{SR_1}x + n_{SR_1} \qquad (10)$$

And the symbol decoded at node R_1 is transmitted to node R_2. The signal received at node R_2 is given as,

$$y_{R_1R_2}^{mmW} = h_{R_1R_2}\tilde{x} + n_{R_1R_2} \qquad (11)$$

After receiving the signal, node R_2 decodes it and subsequently transmits it to node D. Consequently, the signal received at node D is given by,

$$y_{R_2D}^{mmW} = h_{R_2D}\hat{x} + n_{R_2D} \qquad (12)$$

where, $h_{SR_1}, h_{R_1R_2}$ and, h_{R_2D} are S-R_1, R_1-R_2, and R_2-D mm Wave fading channel coefficients respectively. The instantaneous received SNR is given by, $\gamma_j^{mmW} = \bar{\gamma}_j^{mmW}h^2$ where $\bar{\gamma}_j^{mmW}$ is the ASNR of the mm Wave link. The PDF of γ_j^{mmW} follows Gamma distribution [16], and is given by,

$$f_{\gamma_j^{mmw}}(\gamma) = \left(\frac{m}{\bar{\gamma}_j^{mmW}}\right)^m \frac{(\gamma)^{m-1}}{\Gamma(m)} e^{-\frac{m\gamma}{\bar{\gamma}_j^{mmW}}} \qquad (13)$$

Where the function $\Gamma(m)$ denotes the standard Gamma function, and m represents the degree of fading severity in the channel. The cumulative distribution function of γ_j^{mmW} is calculated by integrating its probability density function, resulting in the following expression,

$$F_{\gamma_j^{mmW}}(\gamma) = \int_0^\gamma f_{\gamma_j^{mmW}}(\gamma)\, d\gamma = \frac{1}{\Gamma(m)}\gamma\left(m, \frac{\gamma m}{\bar{\gamma}_j^{mmW}}\right) \qquad (14)$$

Where, $\Upsilon(a, x)$ is the lower incomplete gamma function and is given by,

$$\gamma(a, x) = \int_0^x t^{a-1} e^{-t} dt \qquad (15)$$

3. STATISTICAL PROPERTIES OF THE PROPOSED MULTI-HOP SYSTEM

In this section, we provide the derivation of the cumulative distribution function and probability density function for the proposed system, considering Nakagami-m and Log-Normal fading channels for mm Wave and FSO links, respectively.

3.1 Derivation of cumulative distribution function and probability density function of the proposed system over L-N fading channel

In multi-hop systems, the overall performance is contingent upon the weakest link. The equivalent output SNR (γ_{TH}) is given by [17]

$$\gamma_{TH} = \min_{j=1,2,3} \gamma_j \qquad (16)$$

The CDF of γ_{TH}^{FSO} for multi-hop FSO transmission can be derived as

$$F_{\gamma_{TH}^{FSO}}^{LN}(\gamma) = 1 - \Pr[\gamma_{SR_1}^{FSO} > \gamma_{R_1R_2}^{FSO} > \gamma_{R_2D}^{FSO} > \gamma] \qquad (17)$$

The above equation (17) can be written equivalently over L-N fading channel as

$$F_{\gamma_{TH}^{FSO}}^{LN}(\gamma) = 1 - \prod_j \left[1 - F_{\gamma_j^{FSO}}^{LN}(\gamma)\right] \qquad (18)$$

$F_{\gamma_{TH}^{FSO}}^{LN}(\gamma)$ is the CDF of γ_{TH}^{FSO} over L-N fading channel and is obtained by using *equation (9)* as

$$F_{\gamma_{TH}^{FSO}}^{LN}(\gamma) = 1 - \left[\frac{1}{2}\mathrm{erfc}\left(\frac{\ln\left(\frac{\gamma}{\bar{\gamma}_{SR_1}^{FSO}}\right)+8\sigma_x^2}{\sqrt{32}\sigma_x}\right)\frac{1}{2}\mathrm{erfc}\left(\frac{\ln\left(\frac{\gamma}{\bar{\gamma}_{R_1R_2}^{FSO}}\right)+8\sigma_x^2}{\sqrt{32}\sigma_x}\right)\frac{1}{2}\mathrm{erfc}\left(\frac{\ln\left(\frac{\gamma}{\bar{\gamma}_{R_2D}^{FSO}}\right)+8\sigma_x^2}{\sqrt{32}\sigma_x}\right)\right] \qquad (19)$$

The PDF of γ_{TH}^{FSO} over L-N fading channel is obtained by differentiating $F_{\gamma_{TH}^{FSO}}^{LN}(\gamma)$ with respect to γ and on further simplification it is given by,

$$f_{\gamma_{TH}^{fso}}^{LN}(\gamma) = Ae^{-\frac{\left[\ln\left(\frac{\gamma}{\bar{\gamma}_{SR_1}^{fso}}\right)+8\sigma_x^2\right]^2}{32\sigma_x^2}} + Ae^{-\frac{\left[\ln\left(\frac{\gamma}{\bar{\gamma}_{R_1R_2}^{fso}}\right)+8\sigma_x^2\right]^2}{32\sigma_x^2}} +$$

$$Ae^{-\frac{\left[\ln\left(\frac{\gamma}{\bar{\gamma}_{R_2D}^{fso}}\right)+8\sigma_x^2\right]^2}{32\sigma_x^2}} - Ae^{-\frac{\left[\ln\left(\frac{\gamma}{\bar{\gamma}_{SR_1}^{fso}}\right)+8\sigma_x^2\right]^2}{32\sigma_x^2}}\left[1 - \frac{1}{2}\mathrm{erfc}\left(\frac{\ln\left(\frac{\gamma}{\bar{\gamma}_{R_1R_2}^{fso}}\right)+8\sigma_x^2}{\sqrt{32}\sigma_x}\right)\right]\frac{1}{2}\mathrm{erfc}\left(\frac{\ln\left(\frac{\gamma}{\bar{\gamma}_{R_2D}^{fso}}\right)+8\sigma_x^2}{\sqrt{32}\sigma_x}\right) -$$

$$Ae^{-\frac{\left[\ln\left(\frac{\gamma}{\bar{\gamma}_{R_1R_2}^{fso}}\right)+8\sigma_x^2\right]^2}{32\sigma_x^2}}\left[1-\right.$$

$$\frac{1}{2}\,erfc\left(\frac{\ln\left(\frac{\gamma}{\bar{\gamma}_{R_2D}^{fso}}\right)+8\sigma_x^2}{\sqrt{32}\sigma_x}\right)\right]\frac{1}{2}\,erfc\left(\frac{\ln\left(\frac{\gamma}{\bar{\gamma}_{SR_1}^{fso}}\right)+8\sigma_x^2}{\sqrt{32}\sigma_x}\right)-$$

$$Ae^{-\frac{\left[\ln\left(\frac{\gamma}{\bar{\gamma}_{R_2D}^{fso}}\right)+8\sigma_x^2\right]^2}{32\sigma_x^2}}\left[1-\right.$$

$$\frac{1}{2}\,erfc\left(\frac{\ln\left(\frac{\gamma}{\bar{\gamma}_{SR_1}^{fso}}\right)+8\sigma_x^2}{\sqrt{32}\sigma_x}\right)\right]\frac{1}{2}\,erfc\left(\frac{\ln\left(\frac{\gamma}{\bar{\gamma}_{R_1R_2}^{fso}}\right)+8\sigma_x^2}{\sqrt{32}\sigma_x}\right) \quad (20)$$

3.2 Derivation of Cumulative Distribution Function and Probability Density Function of the Proposed System over Nakagami-m fading Channel

The expression for the CDF of γ_{TH}^{mmW} for mm Wave transmission is given by,

$$F_{\gamma_{TH}^{mmw}}(\gamma) = 1 - \Pr[\gamma_{SR_1}^{mmW} > \gamma_{R_1R_2}^{mmW} > \gamma_{R_2D}^{mmW} > \gamma] \quad (21)$$

The above *equation (21)* can be written as

$$F_{\gamma_{TH}^{mmw}}(\gamma) = 1 - \prod_j \left[1 - F_{\gamma_j^{mmw}}(\gamma)\right] \quad (22)$$

The CDF o f γ_{TH}^{mmW} over Nakagami-m fading channel, denoted as $F_{\gamma_{TH}^{mmw}}(\gamma)$, can be derived by using *equation (14)* as,

$$F_{\gamma_{TH}^{mmw}}(\gamma) = 1\left[\left(\frac{\Gamma\left(m,\frac{\gamma m}{\bar{\gamma}_{SR_1}^{mmW}}\right)}{\Gamma(m)}\right)\left(\frac{\Gamma\left(m,\frac{\gamma m}{\bar{\gamma}_{R_1R_2}^{mmW}}\right)}{\Gamma(m)}\right)\left(\frac{\Gamma\left(m,\frac{\gamma m}{\bar{\gamma}_{R_2D}^{mmW}}\right)}{\Gamma(m)}\right)\right]$$
$$(23)$$

The expression representing the PDF of γ_{TH}^{mmW} is denoted as $f_{\gamma_{TH}^{mmw}}(\gamma)$. It is derived by taking the derivative of $F_{\gamma_{TH}^{mmw}}(\gamma)$ with respect to γ. The mathematical representation of $f_{\gamma_{TH}^{mmw}}(\gamma)$ is as follows:

$$F_{\gamma_{TH}^{mmw}}(\gamma) = \left(\frac{m}{\bar{\gamma}_{SR_1}^{mmW}}\right)^m \frac{(\gamma)^{m-1}}{\Gamma(m)} e^{-\frac{m\gamma}{\bar{\gamma}_{SR_1}^{mmW}}} +$$

$$\left(\frac{m}{\bar{\gamma}_{R_1R_2}^{mmW}}\right)^m \frac{(\gamma)^{m-1}}{\Gamma(m)} e^{-\frac{m\gamma}{\bar{\gamma}_{R_1R_2}^{mmW}}} + \left(\frac{m}{\bar{\gamma}_{R_2D}^{mmW}}\right)^m \frac{(\gamma)^{m-1}}{\Gamma(m)} e^{-\frac{m\gamma}{\bar{\gamma}_{R_2D}^{mmW}}} \quad (24)$$

4. PERFORMANCE ANALYSIS OF THE PROPOSED MULTI-HOP SYSTEM

The formulas for the OP and ABER pertaining to the proposed system, which operates between the source and destination nodes, are obtained in this section. Let's start with the OP expression for the proposed system [18], which is given by,

$$P_{out}^{TH-LN} = F_{\gamma_{TH}^{FSO}}^{LN}(\gamma_{th}^{FSO}) F_{\gamma_{TH}^{mmw}}(\gamma_{th}^{mmW}) \quad (25)$$

where, $F_{\gamma_{TH}^{FSO}}^{LN}(\gamma_{th}^{FSO})$ is obtained by replacing γ with γ_{th}^{FSO} in *equation (19)* and $F_{\gamma_{TH}^{mmw}}(\gamma_{th}^{mmW})$ is obtained by replacing γ with γ_{th}^{mmW} in *equation (23)*. After applying BPSK modulation, the data is subsequently transmitted via either the FSO or the mm Wave links. The assumption is that both links have the same data rate. The equation that represents the bit error rate for BPSK modulation can be expressed as a function of the instantaneous Signal-to-Noise Ratio, as described in reference [18]

$$p(e/\gamma) = 0.5\,erfc(\sqrt{\gamma}) \quad (26)$$

During periods without outages, the calculation of the ABER can be performed by considering the average BER of each separate FSO and mm Wave link. Mathematically, this can be expressed as,

$$\bar{P}_b^{TH-LN} = \frac{B_{TH}^{LN}(\gamma_{th}^{FSO})+F_{\gamma_{TH}^{FSO}}^{LN}(\gamma_{th}^{FSO})B_{TH}^{mmW}(\gamma_{th}^{mmW})}{1-P_{out}^{TH-LN}} \quad (27)$$

Where, P_{out}^{TH-LN} is given by *equation (25)* and $F_{\gamma_{TH}^{FSO}}^{LN}(\gamma_{th}^{FSO})$ is given by *equation (19)* respectively. The ABER of FSO link ($B_{TH}^{LN}(\gamma_{th}^{FSO})$) and mmW link ($B_{TH}^{mmW}(\gamma_{th}^{mmW})$) are given below. The ABER rate of FSO link is determined by averaging the conditional bit error rate of BPSK signal. This averaging is performed over the pdf of γ_{TH}^{FSO}, subject to the condition that $\gamma_{TH}^{FSO} > \gamma_{th}^{FSO}$. The average BER can be expressed as follows,

$$B_{TH}^{LN}(\gamma_{th}^{FSO}) = \int_{\gamma_{th}^{FSO}}^{\infty} p(e/\gamma)\, f_{\gamma_{TH}^{LN}}^{LN}(\gamma)\, d\gamma \quad (28)$$

Where, $p(e/\gamma)$ and $f_{\gamma_{TH}^{FSO}}^{LN}(\gamma)$ are given by *equation (27) & (20)* respectively. The ABER of mm Wave link is determined by averaging the conditional BER of binary phase shift keying signal over the pdf of γ_{TH}^{mmW}. This calculation considers the condition that $\gamma_{TH}^{mmW} > \gamma_{th}^{mmW}$. The mathematical formula for the average BER is expressed as

$$B_{TH}^{mmW}(\gamma_{th}^{mmW}) = \int_{\gamma_{th}^{mmw}}^{\infty} p(e/\gamma)\, f_{\gamma_{TH}^{mmw}}(\gamma)\, d\gamma \quad (29)$$

Where, $p(e/\gamma)$ and $f_{\gamma_{TH}^{mmw}}(\gamma)$ are given by *equation (27)* and *equation (24)* respectively. By substituting *equation (28)* and *equation (29)* in *equation (27)*, the expression for the ABER of the proposed system can be obtained.

5. RESULTS AND DISCUSSION

The efficacy of the proposed system is verified based on the analysis of derived analytical expressions for OP and ABER under various turbulent channel conditions in this section.
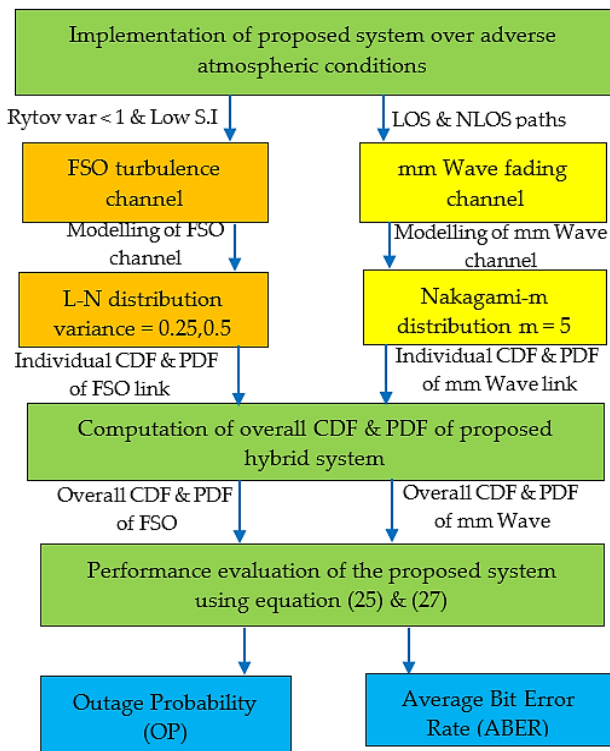
Figure 2: Multi-hop hybrid system implementation over various channel scenarios

Figure 2 illustrates the steps employed in deploying the proposed muti-hop system, utilizing FSO and mm Wave links over turbulent channel conditions. The FSO link is modelled by L-N distribution with variance values of 0.25 and 0.5 over weak turbulence conditions and the mm Wave link is characterized by using a Nakagami-m distribution, where *m* is equal to 5.

5.1 Outage Probability vs Average SNR of Multi-Hop Hybrid System

The OP versus the average SNR for the multi-hop system and FSO-TH, with a fixed threshold value of 5 dB is shown in *figure 3*.
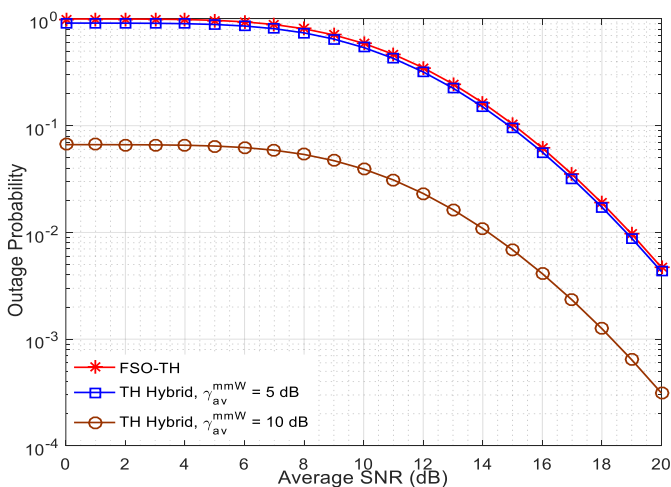

Figure 3: OP performance of the proposed system over various mm Wave links

The varying average SNR suggests the changing weather conditions. From *figure 3*, it becomes apparent that proposed system exhibits superior outage performance in comparison to the FSO alone system, especially in instances where a high-quality mm Wave ($\gamma_{av}^{mmW} = 10$ dB) link is employed. Despite the low-quality mm Wave link ($\gamma_{av}^{mmW} = 5$ dB) the proposed system demonstrates improvement compared to the FSO alone system. As an example, if the average SNR is 10 dB, FSO-TH system demonstrates an OP of 5.9×10^{-1}. However, the proposed system achieves OP values of 5.4×10^{-1} and 3.9×10^2 for various mm Wave links, respectively.

Figure 4 illustrates that the proposed system exhibits superior outage behavior in comparison to FSO-TH system. Nevertheless, as anticipated, the outage performance declines as the value of σ_x increases.
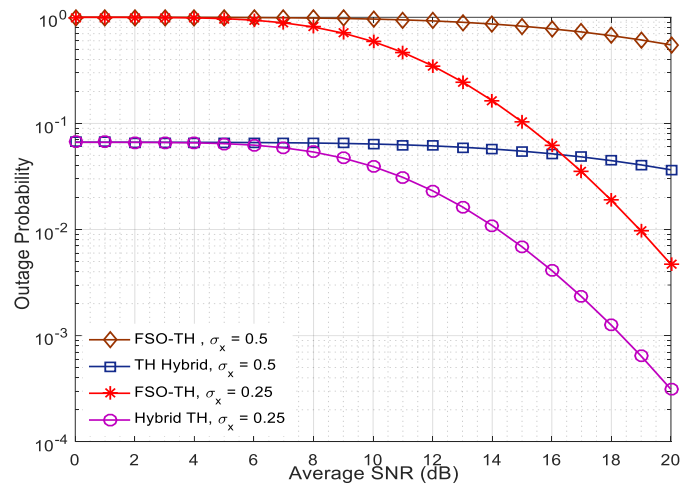

Figure 4: OP performance of the proposed system for various values of σ_x

Table 1 presents the OP values for both the FSO-TH and proposed system, considering various values of σ_x, while utilizing a superior mm Wave link. For example, when the average SNR is 10 dB, the proposed system shows an OP of 3.9×10^{-2} and 6.3×10^{-2} for σ_x values of 0.25 and 0.5, respectively. On the other hand, FSO-TH system demonstrates an OP of 5.9×10^{-1} and 9.6×10^{-1}, for the same σ_x values.

Table 1: OP of proposed system & FSO - TH vs average SNR

S.No.	Avg. SNR (dB)	FSO-TH system		Proposed system	
		$\sigma_x = 0.25$	$\sigma_x = 0.5$	$\sigma_x = 0.25$	$\sigma_x = 0.5$
1	2	9.9×10^{-1}	9.9×10^{-1}	6.6×10^{-2}	6.6×10^{-2}
2	4	9.8×10^{-1}	9.9×10^{-1}	6.5×10^{-2}	6.6×10^{-2}
3	6	9.3×10^{-1}	9.9×10^{-1}	6.2×10^{-2}	6.6×10^{-2}
4	8	8.0×10^{-1}	9.8×10^{-1}	5.3×10^{-2}	6.5×10^{-2}
5	10	5.9×10^{-1}	9.6×10^{-1}	3.9×10^{-2}	6.3×10^{-2}
6	12	3.4×10^{-1}	9.2×10^{-1}	2.3×10^{-2}	6.1×10^{-2}
7	14	1.6×10^{-1}	8.6×10^{-1}	1.0×10^{-2}	5.7×10^{-2}
8	16	6.1×10^{-2}	7.7×10^{-1}	4.1×10^{-3}	5.1×10^{-2}
9	18	1.8×10^{-2}	6.7×10^{-1}	1.2×10^{-3}	4.4×10^{-2}
10	20	4.7×10^{-3}	5.4×10^{-1}	3.1×10^{-4}	3.6×10^{-2}

5.2 Average BER vs Average SNR of Proposed System

The proposed system ABER performance is depicted in *figure 5*, showcasing its relationship with the average SNR for specific threshold value of 5 dB, which remains fixed throughout the analysis. The proposed system enhanced ABER performance in comparison to the FSO-TH system, which can be observed in *figure 5*. The ABER performance shows only a slight enhancement, particularly in the low SNR range, when employing a high-quality mm Wave ($\gamma_{av}^{mmW} = 10$ dB), link. This occurs because the superior mm Wave link is utilized more often in instances where the average SNR of the FSO link is relatively low. With the enhancement of the average SNR in the Free Space Optical connection, the reliance on the FSO link for transmission grows steadily. This results in additional enhancements in the ABER performance of the system under consideration. For example, when considering an average signal-to-noise ratio of 10 dB, the FSO-TH system demonstrates an ABER of 2.0×10^{-2}. However, the proposed system achieves better performance, with ABER of 1.3×10^{-3} and 7.0×10^{-4} with different mm Wave links respectively.
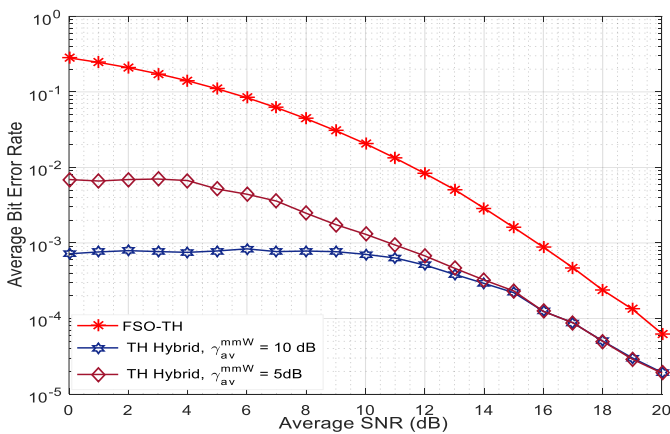

Figure 5: ABER performance of the proposed system over various mm Wave links

Figure 6 depicts the changes in the ABER of the FSO-TH and the multi-hop hybrid system as the average SNR varies, considering different values of σ_x.
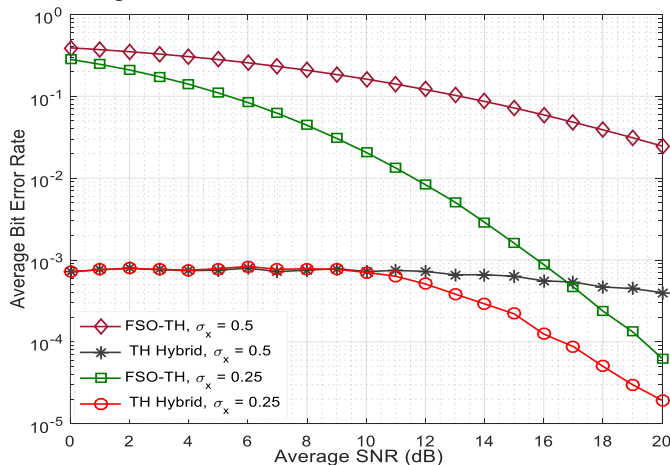

Figure 6: ABER performance of the proposed system for various values of σ_x

The graph presents a distinct illustration of the outstanding performance of the suggested system when contrasted with the FSO-TH system, in terms of average BER.

Table 2 displays the average BER values for different σ_x values, showcasing the system's remarkable performance on a superior mm Wave link. For example, when the average SNR is 10 dB, the Free-Space Optical -TH system demonstrates an average BER of 2.0×10^{-2} and 1.6×10^{-1}, respectively for different σ_x values. In contrast, the proposed system achieves an average BER of 7.0×10^{-4} and 7.2×10^{-4}, for $\sigma_x = 0.25$ and 0.5, respectively.

Table 2: Average bit error rate of proposed system and FSO-TH vs average SNR

S.No.	Avg. SNR (dB)	FSO-TH system		Proposed system	
		$\sigma_x = 0.25$	$\sigma_x = 0.5$	$\sigma_x = 0.25$	$\sigma_x = 0.5$
1	2	2.0×10^{-1}	3.4×10^{-1}	7.9×10^{-4}	7.9×10^{-4}
2	4	1.4×10^{-1}	3.0×10^{-1}	7.5×10^{-4}	7.4×10^{-4}
3	6	8.3×10^{-2}	2.5×10^{-1}	8.3×10^{-4}	7.9×10^{-4}
4	8	4.4×10^{-2}	2.0×10^{-1}	7.8×10^{-4}	7.5×10^{-4}
5	10	2.0×10^{-3}	1.6×10^{-1}	7.0×10^{-4}	7.2×10^{-4}
6	12	8.3×10^{-3}	1.2×10^{-1}	5.1×10^{-4}	7.2×10^{-4}
7	14	2.8×10^{-3}	8.6×10^{-2}	2.9×10^{-4}	6.6×10^{-4}
8	16	8.7×10^{-4}	5.9×10^{-2}	1.2×10^{-4}	5.5×10^{-4}
9	18	2.3×10^{-4}	3.8×10^{-2}	5.0×10^{-5}	4.6×10^{-4}
10	20	6.3×10^{-5}	2.4×10^{-2}	1.9×10^{-5}	4.0×10^{-4}

6. CONCLUSION

In this paper, we present an analysis of a multi-hop hybrid system that combines Free-Space Optical and millimeter Wave technologies. The system utilizes decode and forward relaying, along with selection combining, to enhance performance. Our investigation focuses on evaluating the system's outage probability and average bit error rate using both analytical expressions and Monte-Carlo simulations. To model the FSO link, we adopt a Log-Normal distribution with variance values of 0.25 and 0.5. The mm Wave link, on the other hand, is represented by a Nakagami-m distribution with m = 5. By analyzing the results, it can be concluded that the proposed system, with selection combining, outperforms FSO-only systems under various channel conditions. This superior performance can be attributed to the benefits of diversity and switching within the hybrid system. Consequently, the suggested system shows significant potential for next-generation wireless networks, enabling seamless provision of high-bandwidth services like 5G and beyond, in both urban and rural environments.

REFERENCES

[1] Al-Gailani, S. A.; Mohd Salleh, M. F.; Salem, A. A.; Shaddad, R. Q.; Sheikh, U. U.; Algeelani, N. A.; & Almohamad, T. A. A Survey of Free Space Optics (FSO) Communication Systems, Links, and Networks. IEEE Access, 2021, 9, 7353–7373.

[2] Abdalla, A.M.; Rodriguez, J.; Elfergani, I.; Teixeira, A. Optical and Wireless Convergence for 5G Networks; John Wiley & Sons: Hoboken, NJ, USA, 2019.

[3] Magidi, S.; Jabeena, A. Free Space Optics, Channel Models and Hybrid Modulation Schemes: A Review. Wirel. Pers. Commun., 2021, 119(4), 2951–2974.

[4] Wu, Y.; Mei, H.; Dai, C.; Zhao, F.; Wei, H. Design and analysis of performance of FSO communication system based on partially coherent beams. Opt. Commun. 2020, 472, 1–7.

[5] Shakir, W.M.R. Performance evaluation of a selection combining scheme for the hybrid FSO/RF system. IEEE Photonics Journal 2017, 10, 1–10.

[6] Tahami, A.; Dargahi, A.; Abedi, K.; Chaman-Motlagh, A. A new relay-based architecture in hybrid RF/FSO system. Phys. Commun. 2019, 36, 1–9.

[7] Wu, Y.; Chen, J.; Guo, J.; Li, G.; Kong, D. Performance Analysis of a Multi-Hop Parallel Hybrid FSO/RF System over a Gamma—Gamma Turbulence Channel with Pointing Errors and a Nakagami-m Fading Channel. Proc. Photonics 2022, 9, 631.

[8] Vishwakarma, N.; Swaminathan, R. Performance analysis of hybrid FSO/RF communication over generalized fading models. Opt. Commun. 2021, 487, 126796.

[9] Vishwakarma, N.; Swaminathan, R. On the Capacity Performance of Hybrid FSO/RF System with Adaptive Combining Over Generalized Distributions. IEEE Photonics J. 2021, 14, 1–12.

[10] Liang, H.; Gao, C.; Li, Y.; Miao, M.; Li, X. Analysis of selection combining scheme for hybrid FSO/RF transmission considering misalignment. Opt. Commun. 2019, 435, 399–404.

[11] Alathway, W.A.; Altubaishi, E.S. On the performance analysis of decode-and-forward multi-hop hybrid FSO/RF systems with hard-switching configuration. IEEE Photonics J. 2019, 11, 1–12.

[12] Khalid, H.; Muhammad, S.S.; Nistazakis, H.E.; Tombras, G.S. Performance analysis of hard-switching based hybrid FSO/RF system over turbulence channels. Computation 2019, 7, 28

[13] Odeyemi, K.O.; Owolawi, P.A. Selection combining hybrid FSO/RF systems over generalized induced-fading channels. Opt. Commun. 2019, 433, 159–167.

[14] Amirabadi, M.A.; Vakili, V.T. Performance comparison of two novel relay-assisted hybrid FSO/RF communication systems. IET Commun. 2019, 13, 1551–1556.

[15] Usman, M.; Yang, H.-C.; Alouini, M.-S. Practical Switching-Based Hybrid FSO/RF Transmission and Its Performance Analysis. IEEE Photonics J. 2014, 6, 1–13.

[16] Sharma, S.; Madhukumar, A.; Swaminathan, R. Switching-based cooperative decode-and-forward relaying for hybrid FSO/RF networks. J. Opt. Commun. Netw. 2019, 11, 267–281.

[17] Wang, P.; Wang, R.; Guo, L.; Cao, T.; Yang, Y. On the performances of relay-aided FSO system over M distribution with pointing errors in presence of various weather conditions. Opt. Commun. 2016, 367, 59–67.

[18] Usman, M.; Yang, H.C.; Alouini, M.S. Practical switching-based hybrid FSO/RF transmission and its performance analysis. IEEE Photonics J. 2014, 6, 1–13.

[19] Gradshteyn I. S, and Ryzhik I. M. Table of Integrals, Series, and Products. 8th ed. Elsevier Acadimic Press.